Electronic Supplementary Information (ESI†)

Gemini basic ionic liquid and functionalized cellulose nanocrystal based mixed matrix membrane for CO_2/N_2 separation

[a,b]*Prarthana Bora,* [a,b]*Chinmoy Bhuyan,* [a,b]*Parashmoni Rajguru,* [a,b]*Swapnali Hazarika**

[a]*Chemical Engineering Group and Centre for Petroleum Research*

CSIR-North East Institute of Science and Technology, Jorhat – 785006, Assam, India

Phone: ++913762370012, Email: shrrljt@yahoo.com

[b]*Academy of Scientific and Innovative Research (AcSIR), Ghaziabad-201002, India*

*Author for correspondence

Table of Contents:

Experimental

Materials

Cellulose nanocrystals used in the study has been obtained from waste napkin papers available in our laboratory by acid hydrolysis. Thionyl chloride, N, N-dimethylformamide, 1-bromooctane and 1, 2-dibromobutane used in the study are obtained from SRL Private Limited, India. Potassium hydroxide and N-methyl-pyrrolidone have been purchased from Emplura^{R}, Merck Life Science Private Limited, India. Ethane-1, 2-diamine used in this study is obtained from Tokyo Chemical Industry Co. Limited. Polysulfone (Molecular weight 60000) has been obtained from ThermoFisher Scientific India Pvt. Ltd., Morpholine is obtained from Molychem, Mumbai, India. Ethanol used in the study is purchased from Spectrochem Private Limited, Mumbai, India. 99% pure CO_2 and N_2 used in the study have been supplied by Gas Centre, AT Road, Tarajan, Jorhat, Assam.

Characterizations

Perkin Elmer FTIR instrument has been used to know the functional group present in the synthesized IL, CNC, functionalized CNC and membranes with ATR and without ATR mode (liquid with $CHCl_3$ solvent) in the spectral range of 4000-400 cm^{-1} with 16 scans. The ^{1}H and ^{13}C NMR analysis of synthesized IL has been done in Bruker 400 MHz NMR spectrometer with $CDCl_3$ as solvent. Thermal stability has been observed using Perkin Elmer 4000 instrument in the temperature range 35-600 ºC at a heating rate of 10 ºC/min in nitrogen environment. Morphological analysis of the membrane surfaces has been done by with field emission scanning electron microscope (Carl Zeiss Sigma VP microscope). The membranes are cut into 2 mm × 2 mm dimensions and are dried at room temperature in vacuum drier and dipped in liquid nitrogen prior to the analysis. Membrane surface roughness has been analysed by Atomic Force Microscope, Oxford instrument of Cypher model. The mechanical property

of the membranes has been done by a universal testing machine ("Tinius Olsen 5ST" model) using a load cell of 2.5 kN and testing speed 5mm/min. The pore size distribution of the membranes have been done with a BET analyzer (Quantachrome Instruments version 5.21) applying the degassing temperature at 100ºC using XeriPrep degasser and under vacuum. Thermo Fisher Scientific ESCALAB Xi+ instrument has been used for XPS analysis. Refinery Gas Analyzer (RGA) of model-8890GC system of Agilent company has been used for gas chromatographic analysis of the permeate gas mixture.

Synthesis of Gemini basic ionic liquid [Nbmd][OH]

Two steps have been involved in the synthesis of Gemini dibasic ionic liquid. The synthesis has been done by the method reported earlier[1,2]. Firstly, the addition of 1-bromooctane with NaOH has been done and put in a dry round bottom flask connected with a condenser. The mixture is allowed to heat at 40 ºC followed by dropwise addition of morpholine-water solution which is preheated at 70 ºC. The reaction mixture with molar ratio of $n_{1\text{-bromooctane}} : n_{morpholine} : n_{NaOH} : n_{H2O}$ = 1:1.2:1.5:5 is stirred in a magnetic stirrer under reflux condition at 130 ºC for 7 h. After 7 h the reaction mixture has been allowed to attain room temperature. The resultant solution gives a two layers system from where the clear upper layer has been collected with the help of a separating funnel. The collected solution is the intermediate product octyl morpholine.

The amount of octyl morpholine obtained in the 1st step has been taken as a starting material in the 2nd step and placed in a dry round bottom flask. 1,4-dibromobutane has been added to the flask in a molar ratio of $n_{\text{octyl morpholine}} : n_{\text{1,4-dibromobutane}}$ = 2:1 and allowed the reaction to run under reflux condition at 110 ºC for 7 h in a magnetic stirrer. A yellowish sticky viscous product of bromooctyl morpholine is obtained which has been dried for 24 h at 50 ºC under vacuum. The given amount of dry product obtained has been taken in a conical flask, then KOH is added at a molar ratio of $n_{\text{bromooctyl morpholine}} : n_{KOH}$ =1:2 and anhydrous ethanol is taken as a solvent.

The whole reaction mixture is then stirred continuously at room temperature for 48 h. This step is important since it will allow to occur ion exchange. KBr will precipitated out as white solid and is separated via centrifuge (10000 rpm, room temperature). From the solution, the solvent has been evaporated in a rotary evaporator at 60 ºC and the ionic liquid is obtained which termed as [Nbmd][OH] (4,40-(butane-1,4-diyl)bis(4-octyl-morpholin-4-ium)hydroxide). Characterization such as FT-IR, NMR and HRMS of the synthesized ionic liquid have been done.

Synthesis of cellulose nanocrystal (CNC)

Tissue paper has been used as the source material for cellulose. Sulfuric acid based hydrolysis of cellulose is a commonly used method which is utilized in this study[3]. Herein the synthesis comprises of three consecutive steps. At the very 1st stage, 10 g of tissue papers have been cut into small (approximately 2 cm^3) pieces and are taken in a round bottom flask. The same has been treated with 200 ml 0.5 N NaOH and stirred on a magnetic stirrer for two hours at 80 ºC temperature under reflux condition. The base treated cellulose has been washed vigorously with distilled water for neutralization. After neutralization, in the 2nd step the cellulose has been subjected to acid treatment where 200 ml of 0.5 N HCl solution is added to the cellulose content in a round bottom flask and stirred for 2 hours at 80 ºC under reflux. The acid treated cellulose has been washed again with distilled water until neutralization point has been achieved. The last step is the acid hydrolysis step where cellulose has been treated with 64% (w/w: 56.4 ml H_2SO_4 in 55.4 ml H_2O) H_2SO_4 at 50 ºC for 3 hours. The hydrolysed product has been first neutralized and then extracted via centrifugal separation for further processing.

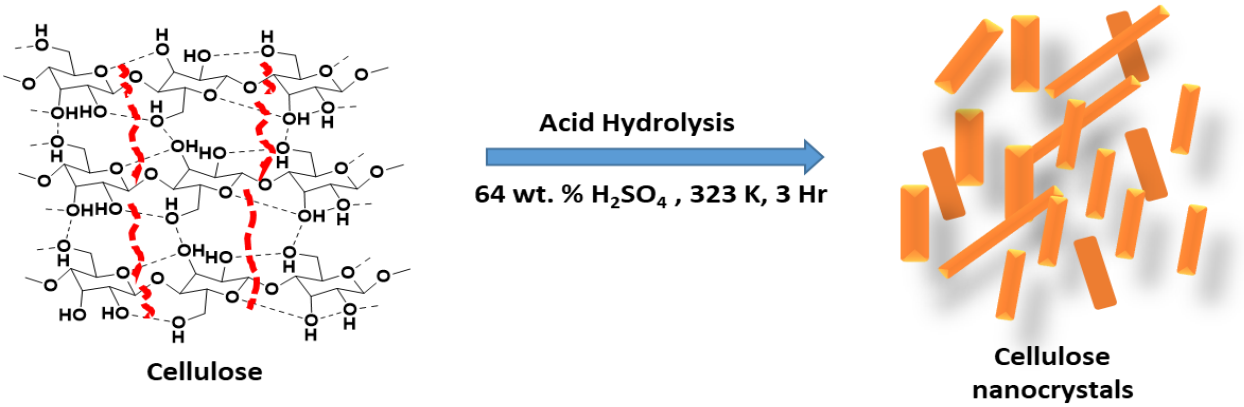

Figure S1: Representation of cellulose to cellulose nanocrystal conversion

Functionalization of cellulose nanocrystal

Functionalization of cellulose nanocrystal has been carried out following a reported method containing two step synthesis[4]. 2 g of cellulose nanocrystal has been taken in a round bottom flask with 40 ml of N, N-dimethyl-formamide (DMF) as solvent and 7 ml of $SOCl_2$ has been added slowly while stirring at 80 ºC. The reaction has been allowed to run for 4 hours at the same temperature. The produced cellulose chloride (CNC-Cl) is kept to attain room temperature and washed with dilute ammonium hydroxide solution 4-5 times to attain neutral condition followed by washed with distilled water several times. The product has been collected through centrifugal separation. 2 g of cellulose chloride has been taken in a round bottom flask and 10 ml of ethane-1, 2-diamine is added and stirred for 3 hours in a mechanical stirrer under reflux condition. After completion of the reaction the resultant CNC-NH_2 has been collected via centrifuging at 10000 rpm and 25 ºC.

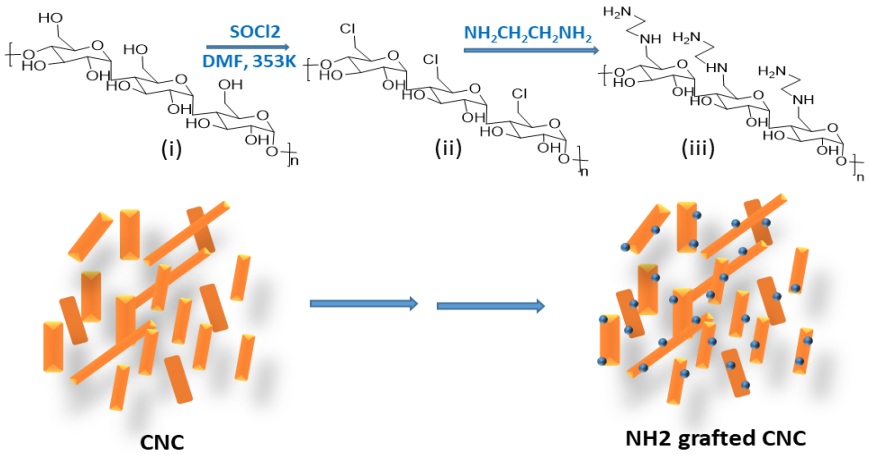

Figure S2: Synthesis route of cellulose nanocrystal to amine grafted cellulose nanocrystal

Preparation of Polysulfone/CNC-NH_2/[Nbmd][OH] mixed matrix membrane

A CO_2 selective membrane made of polysulfone and amine functionalized cellulose nanocrystal incorporated with dual core ionic liquid has been designed. Waste tissue papers has been taken as the source for synthesis of cellulose nanocrystal. The unique idea of using dual core ionic liquid with morpholinium cationic core instead of imidazolium and hydroxyl anion has been endeavored in this work. The scheme for membrane fabrication is demonstrated in Scheme S1.

0.23 % (w/v) polysulfone (PSF) solution with NMP as solvent (23 g polysulfone in 100 ml NMP) has been prepared via magnetic stirring at 60 ºC for 6 hours. After complete dissolution of PSF, CNC-NH_2 (concentration as shown in Table S1) has been added to the solution while stirring. After 1 hour of stirring at room temperature homogeneous solution has been obtained. 4 ml of the prepared ionic liquid [Nbmd][OH] is added to the homogeneous solution and has been dispersed thoroughly. After 2 hours of continuous stirring at room temperature, the solution has been kept at stand by for 2 hours to remove the bubbles. A glass plate has been taken on which the solution is poured and sprayed via a glass rod. For maintaining homogeneous thickness of the membrane, wrapped the two side of the glass rod with 10 cm length of Teflon. The sprayed solution has been kept in air for 30 seconds for evaporation

before dipping the glass plate into a water bath as a non-solvent. The membrane obtained via non-solvent induced phase separation has been named as PCIL0. Other membranes, neat polysulfone membrane (0.23% w/v), polysulfone/CNC-NH_2 membrane and polysulfone/[Nbmd][OH] have been prepared by the same method and named as P, PC and PIL respectively. PCIL1 and PCIL2 membranes have been prepared varying the concentrations of CNC-NH_2 as shown in Table 1. One membrane with 0.1% (w/v) CNC-NH_2 and 4 ml of IL content has been prepared but due to less mechanical strength of 0.92 MPa (as evidence from the Figure S12 in the supplementary document), PCIL2 with 0.8% (w/v) has been taken as the optimized membrane. To achieve higher selectivity, we have further modified the membrane via spray coating of IL instead of blending. We have cut out a circular membrane of area 30 cm^2 made up of polysulfone and CNC-NH_2 blending. 1 ml of IL is dissolved in ethanol with a ratio of 1:9 (IL:EtOH). In a spray bottle the solution of IL is taken and sprayed onto the membrane surface while allowing slow evaporation of ethanol. This membrane is named as PC@IL. The composition of this membrane is given in Table S1.

Table S1: Membranes and respective compositions

Membrane	Composition				
	Polysulfone % (w/v) A	CNC-NH_2 %(w/v) B	[Nbmd][OH] (ml) C	NMP (ml)	Preparation techniques
P	0.23	-	-	100	NIPs
PC	0.23	0.04	-	100	Blending (A+B)/ NIPs
PIL	0.23	-	4	100	Blending(A+C)/ NIPs
PCIL0	0.23	0.04	4	100	Blending(A+B+C)/ NIPs
PCIL1	0.23	0.06	4	100	Blending(A+B+C)/ NIPs

PCIL2	0.23	0.08	4	100	Blending(A+B+C)/ NIPs
PC@IL	0.23	0.08	4	100	Blending(A+B)/ NIPs/ Spray coating(C)

NIPs: Non-solvent induced phase separation

NMP: N-methyl pyrollidone

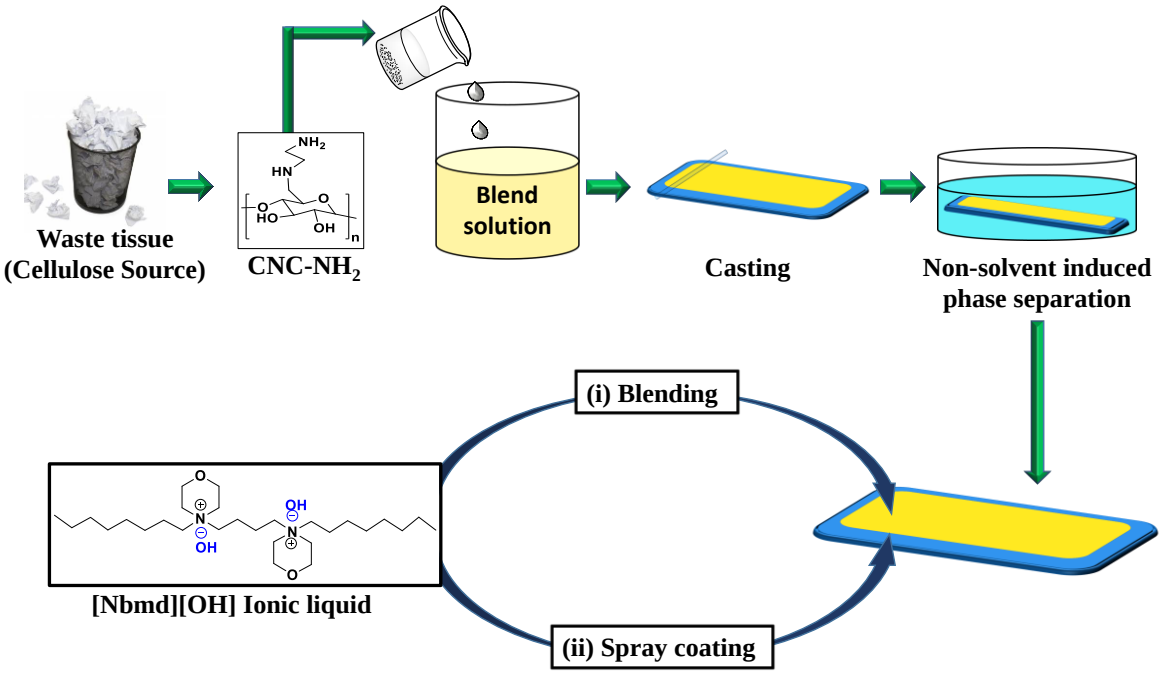

Scheme S1: Schematic representation of Polysulfone/CNC-NH_2/ [Nbmd][OH] membrane fabrication.

Gas permeation theory

The permeance of membrane is the measure of gas permeated through the membrane per unit area per unit time. Here, thickness of the membrane also considered while calculating permeance and can be written as Equation S1. Permeance (Pc) is calculated in unit GPU (1 GPU=10^{-6} cm^3 (STP)/cm^2 s cmHg).

$$Pc = \frac{Q\ (STP)}{A \times \Delta p} \qquad \text{S1}$$

Where, Q (STP) is the volume of the permeate [cm^3], A is the effective membrane area [cm^2], Δp is the difference of the feed pressure and permeate pressure [cmHg].

The permeability of a gas is the rate of gas permeation occurred through the membrane. Permeability of gas through a membrane can be defined as the ease at which gas flows after interaction with membrane material from feed to permeate side. The permeability of membrane can be measured by following Equation S2,

$$P = \frac{Q\ (STP) \times t}{A \times \Delta p} \qquad \text{S2}$$

Here, P stands for the permeability and Q (STP) is the volumetric flow rate (cm^3) at standard pressure and temperature. A is the membrane effective area (cm^2) while Δp stands for the pressure difference (cmHg) over both side of the membrane. And t is the thickness of the membrane (cm). The permeability is measured in common unit Barrer. (1 barrer =$10^{-10}$$cm^3$(STP).cm/($cm^2$.s. cmHg))

The ideal selectivity or separation factor for a gas pair can be expressed as the ratio between their individual permeability as shown in Equation S3.

$$\propto ij\ = \frac{Pi}{Pj} \qquad \text{S3}$$

In Equation S3, 'α_{ij}' is the selectivity of gas 'i' over gas 'j' and P_i and P_j are permeabilities of gas 'i' and 'j' respectively. Following Equation S3 we can calculate the selectivity of a target gas.[5] The ratio of the permeabilities of CO_2 and N_2 will give the CO_2/N_2 selectivity. The more is the gap between their individual permeabilities, the more will be ratio of between them and hence selectivity will increase.

Gas separation experiment

A gas separation set up has been prepared with plate and frame flat sheet membrane module as shown in Scheme S2. For the experiment, gaseous mixture of CO_2 and N_2 in the ratio 50:50

has been taken. The prepared membranes are cut into circular shape of area (28.26 cm^2) to fit properly in the module. The circularly cut membrane with a support was fixed inside the membrane cell. Both the gases have been allowed to pass through the membrane at varying pressure of 1, 2, 3 and 4 bar. The permeate gas is collected in a steel gas collector at the sampling point in a time interval of 1 hour. The collector containing the permeate is removed from the pipe and subjected for gas chromatography (GC) analysis. The same procedure has been repeated in case of each membrane and permeate is collected and analyzed in GC. This procedure has been followed for calculation of permeate concentration. The permeability measurement of each gases viz. CO_2 and N_2 have been done individually. The individual feed gas has been passed through each membrane at varying pressure and flowrate. The inlet and outlet pressures are measured with a pressure gauge and a flowmeter is attached for flowrate measurement. The ball valves have been used for regulating the opening and closing of gas cylinders. By knowing the volumetric flow rate and inlet and outlet pressure we can measure permeance for each gas using Equation S1. Argon has been used as a sweep gas after each permeation to avoid unwanted outcome. The feed stream is not circulated in fact it is a batch process where permeated and retentate gases are collected separately in gas collector. Concentration polarization can be overcome by increasing the feed flow rate. We have performed the individual gas permeation experiment at high flow rate of 800 cm^3/min which shows high permeability referring absence of concentration polarization. In mixed gas permeation at low flow rate, permeability is relatively low corresponding to concentration polarization.

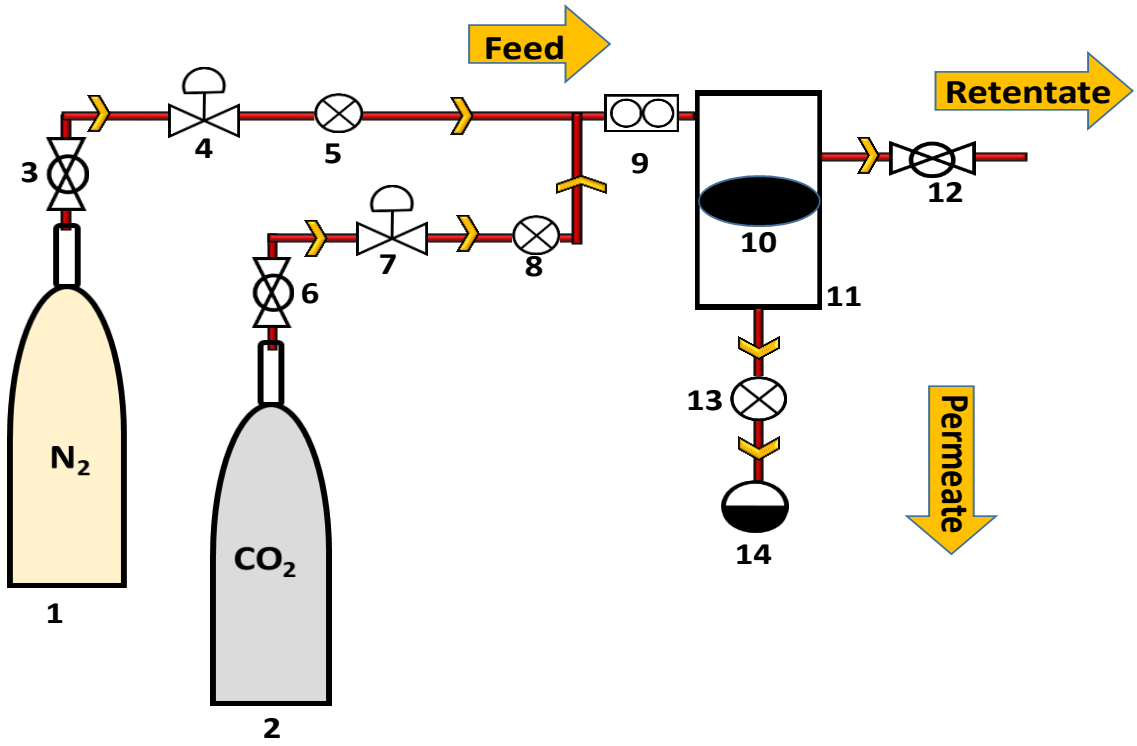

Scheme S2: A schematic representation of permeation set up; 1: N_2 gas cylinder; 2: CO_2 gas cylinder; 3, 6, 12: Ball valve; 4, 7: Pressure regulator; 5, 8, 13: Pressure gauge; 9: Flow meter; 10: Membrane 11: Membrane cell; 14: Sample collection point (to GC).

Characterizations of CNC and CNC-NH_2

CNC has been synthesized in this study from cellulose where waste tissue is used as a cellulose feedstock. The FTIR spectra of CNC and CNC-NH_2 are shown in Figure S3. After amine functionalization of CNC, band at 882 cm^{-1} almost disappears or peak size decreases which is due to the substitution of hydroxyl group by ethane- 1, 2- diamine. The appearance of sharp bands at 2898 cm^{-1} can be explained as C-H stretching frequency which obtained due to CH groups of ethylamine chain[4]. The presence of angular deformation band of N-H at around 1682 cm^{-1} prove that these occurs due to the successful incorporation of amine moiety in CNC structure. The bands at 1632 cm^{-1} and 1638 cm^{-1} is due to O-H bending frequency. Band at 3400 cm^{-1} of CNC is due to the O-H stretching and intermolecular H-bonding[4]. While wide peak obtained at 3391cm^{-1} can be explained as the overlapping O-H and N-H stretching

vibrations. The X-ray photoelectron spectroscopic analysis of functionalized CNC has been done and result obtained are shown in Figure S4. The survey spectra of CNC-NH_2 from Figure shows the corresponding peak for the binding energies of oxygen 1s, nitrogen 1s and carbon 1s orbitals. Deconvoluted high resolution scan for C1s shows that peaks at 288 eV, 286.4 eV, 284.9 eV and 283.7 eV are obtained which are responsible for C-O, C-N, C-C and C-H carbons respectively. From O1s high resolution spectra, peaks a 533.2 eV, 532.6 eV and 531.9 eV are witnessed which are due to the oxygen present in C-O-C, C-O-H and O-H groups respectively. The presence of nitrogen is already witnessed in survey spectra which shows a successful amine group functionalization. Now deconvolution of high-resolution scan of nitrogen gives peak at 402.15 eV, 400.55 eV and 399.45 eV that represents the binding interactions of C-N-C, N-C and N-H groups respectively. Thermal analysis of the synthesized CNC and CNC-NH_2 have been done via thermogravimetric analysis as shown in Figure S5. The first weight loss at around 100 ºC is because of the water molecules bounded loosely to the CNC and CNC-NH_2. Then the 2nd weight loss of CNC occurred at 260 ºC which corresponds to the cellulose moiety decomposition. While in case of CNC-NH_2, the weight loss occurred at 237 ºC which is due to the incorporated ethane-1, 2-diamine decomposition as well as the hydroxyl group decomposition[4]. The nano-range structure of the CNC has been proved with the help of FESEM analysis as shown in Figure S6.

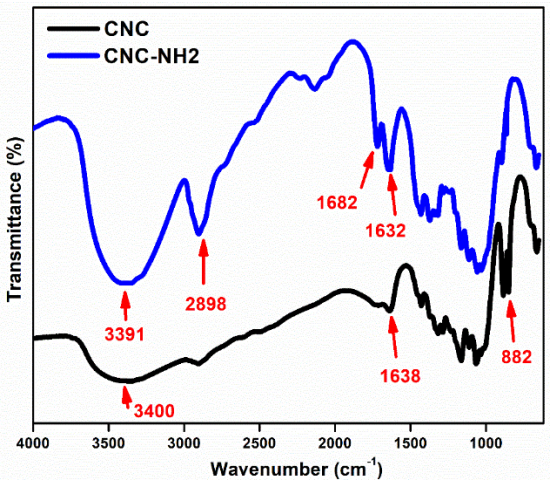

Figure S3: Comparative FTIR analysis of CNC & CNC-NH_2

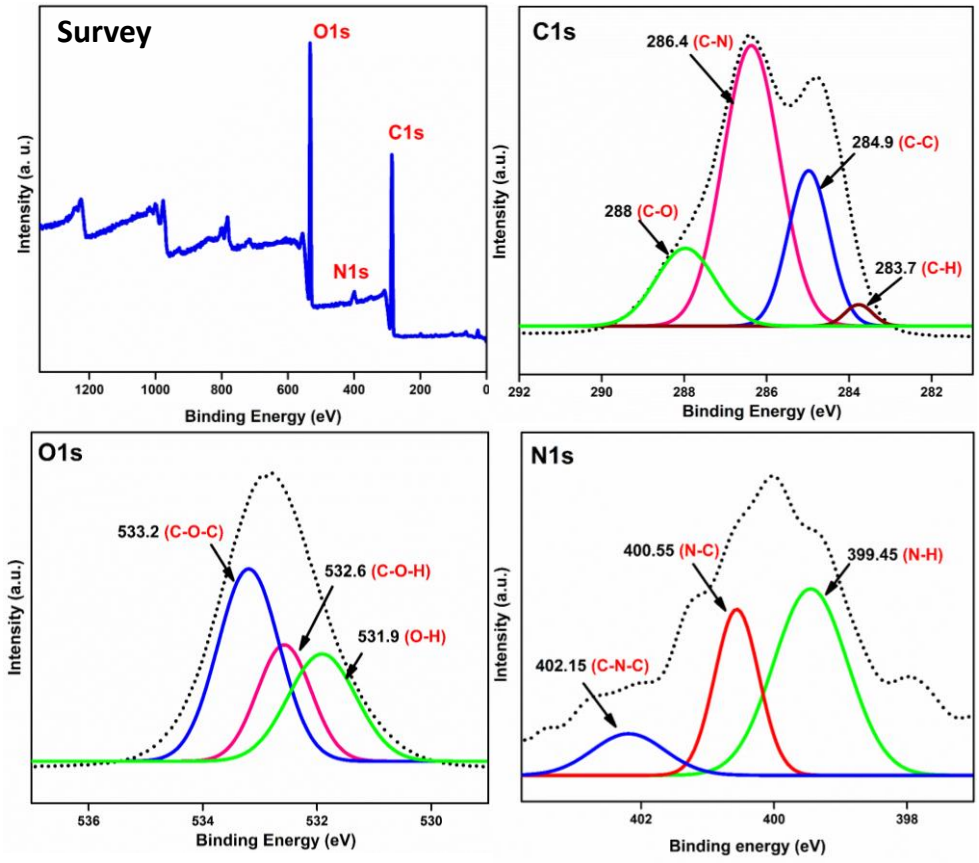

Figure S4: XPS survey and high resolution deconvoluted scan of C1s, O1s & N1s of CNC-NH_2

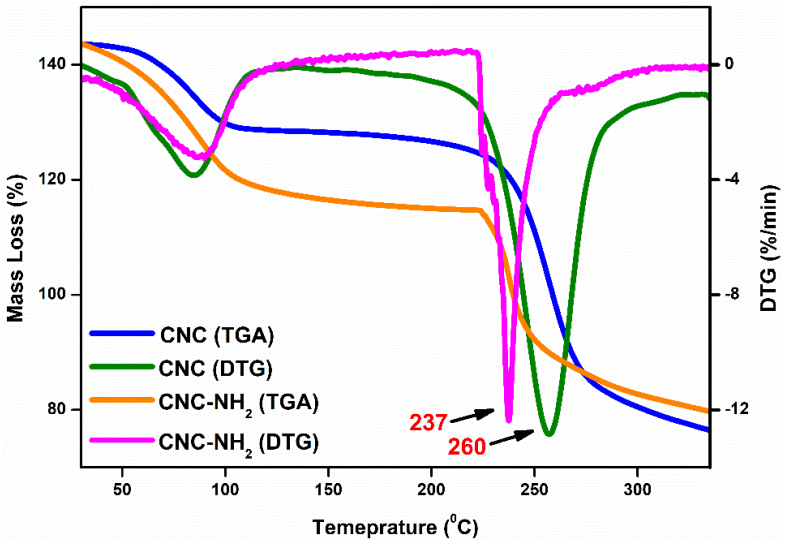

Figure S5: Comparative TGA and DTG analysis of CNC & CNC-NH_2

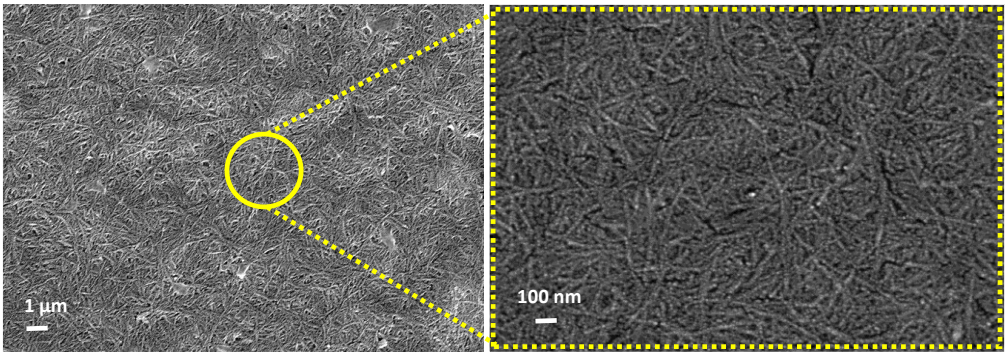

Figure S6: FESEM images of CNC at different diameter ranges

Characterizations of synthesized ionic liquid [Nbmd][OH]

The solubility of the synthesized ionic liquid has been tested in different common solvents and the results are listed in Table S2. The solvents that have been used in this study are N-methyl pyrollidone and water while ionic liquid [Nbmd][OH] showed solubility in both the solvents. As explained in the experimental section, [Nbmd][OH] has been first dissolved in dope solution containing polysulfone and CNC-NH_2 in N-methyl pyrollidone. Here ionic liquid got attached to the CNC-NH_2 and polysulfone via some non-covalent interaction such as hydrogen bonding, van der wall interaction, polar-π and cation-π interactions. Due to presence of these interactions [Nbmd][OH] got attached inside the polymer matrix and couldn't leach out in the water media during non-solvent induced phase separation process. The presence of ionic liquid even after phase inversion has been proved in the XPS study of PIL membrane as shown in Figure S10, where presence of nitrogen can be witnessed.

Table S2: Solubility of [Nbmd][OH] in different solvents

Sl. No.	Ionic liquid	Solvent	Solubility
1	[Nbmd][OH]	Ethyl acetate	-
2		H_2O	+
3		Ethanol	+
4		Methanol	+

5		N-methyl pyrollidone	+
6		Dichloromethane	+
7		Ether	-

[a] + is soluble and – is insoluble

The synthesized ionic liquid has been characterized via different techniques such as FT-IR, ^{1}H NMR, ^{13}C NMR and TGA. The FT-IR study of synthesized ionic liquid [Nbmd][OH] is done and the spectra obtained has been shown in Figure S7. The stretching vibration corresponding to O-H group appeared at 3396 cm^{-1}, which indicates the presence of remaining ethanol. The bands at 2925 cm^{-1} and 2855 cm^{-1} corresponds to the stretching frequency of saturated C-H group. At 1456 cm^{-1}, 1119 cm^{-1} and 1051 cm^{-1} three peaks are obtained which are assigned to some characteristic groups such as vibration frequency of alkane $–CH_2$ deformation, C-O-C stretching and C-N-C stretching present in morpholine ring respectively[1,2]. For the long alkyl chain present in the ionic liquid, a peak at 725 cm^{-1} is observed.

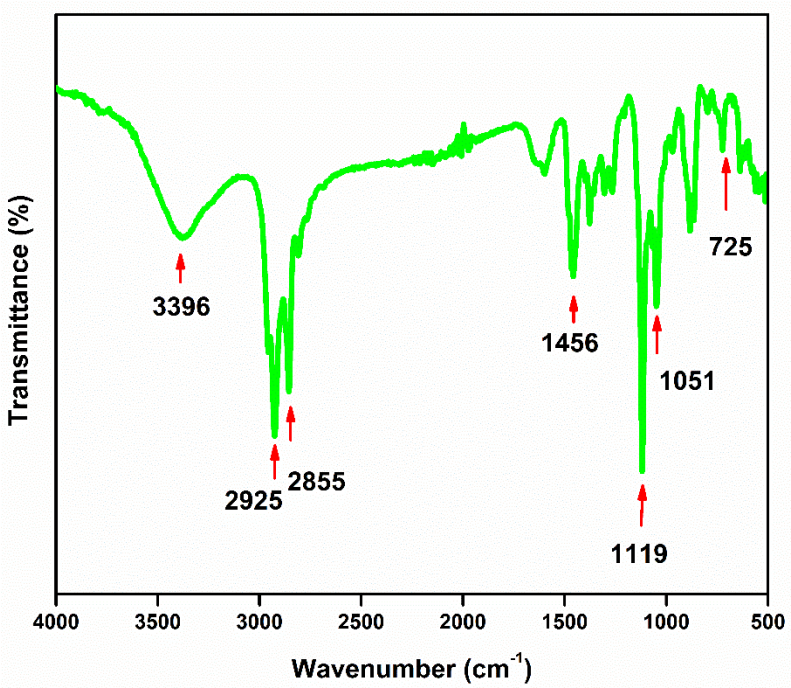

Figure S7: FT-IR spectra of synthesized ionic liquid [Nbmd][OH]

The ^{1}H and ^{13}C NMR analysis of the synthesized ionic liquid have been done ($CDCl_3$, 400 MHz, TMS, ppm) (Figure S8). Consistent values of hydrogen proton numbers and position are obtained with values such as a = 0.70 (6H, $-CH_3$), b = 1.14 (16H, - $(CH_2)_4$-), c = 1.7 (4H, $-CH_2$-), d = 1.8 (4H, $-CH_2$-), g = 1.95 (4H, $-CH_2$-), h = 4.04 (8H, $-CH_2$-), e = 7.28 (4H, $-CH_2$-), f = 7.34 (4H, $-CH_2$-), i = 8.57 (8H, $-CH_2$-). The obtained spectra is comparable to that obtained in the reported study [1]. For 13C NMR, a = 21.55 (2C, $-CH_3$) , b = 22.67 (2C, $-CH_2$-), c = 26.39 (2C, $-CH_2$-), d = 26.59 (2C, $-CH_2$-) , e = 27.60 (2C, $-CH_2$-), f = 29.13 (2C, $-CH_2$-) , g = 29.59 (2C, $-CH_2$-) , j = 31.74 (2C, $-CH_2$-) , h= 53.85 (2C, $-CH_2$-) , k = 59.19 (4C, $-CH_2$-), i =59.61(2C, $-CH_2$-), l = 66.12 (4C, $-CH_2$-) are obtained and are consistent with the carbon number as well as their positions[1,2]. A strong peak at 77.17 is obtained for the solvent $CDCl_3$.

(A)

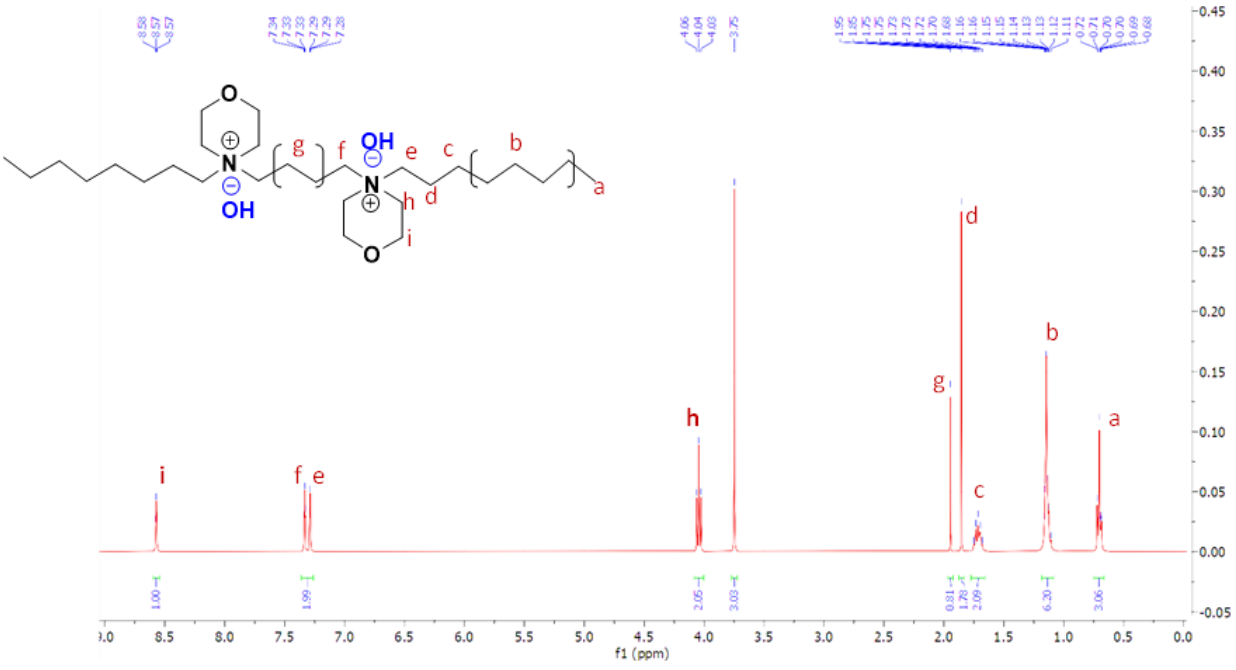

(B)

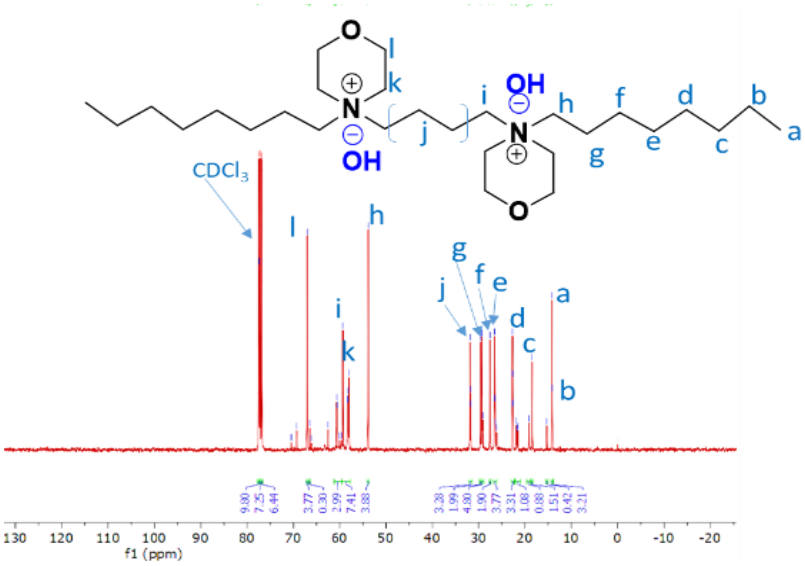

Figure S8: (A) ^{1}H NMR (B) ^{13}C NMR spectrum of synthesized ionic liquid [Nbmd][OH]

The thermal stability of the synthesized ionic liquid [Nbmd][OH] is done by TGA analysis which has been shown in Figure S9. In the temperature range from 235.5 ºC to 345.5 ºC, the weight loss is observed which corresponds to the ionic liquid decomposition. Thus we can say that the synthesized ionic liquids have a high temperature resistance.

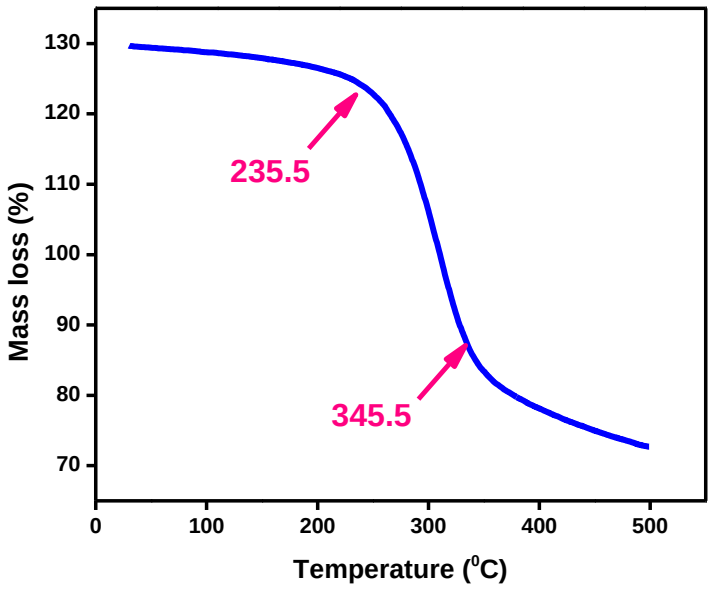

Figure S9: TGA study of synthesized ionic liquid [Nbmd][OH]

Characterizations of the prepared membranes

A total of six membranes have been fabricated viz. P, PC, PIL, PCIL0, PCIL1 and PCIL2. Here P is the bare polysulfone membrane, PC is the polysulfone membranes with CNC-NH_2. PIL, PCIL0, PCIL1 and PCIL2 represents polysulfone/CNC-NH_2/[Nbmd][OH] membrane with varying CNC-NH_2 amount of 0, 0.04, 0.06 and 0.08 % (w/v). The membranes have been prepared using non-solvent induced phase separation which has been illustrated in the experimental section. While fabricating membrane thickness has been kept fixed around 150 ± 10 μm. The produced membranes have been characterized with different analytical techniques such as FESEM and AFM for surface morphology and roughness studies, FTIR for functional group determination, tensile strength for obtaining the mechanical strength of the membranes, TGA and DTG for knowing thermal behaviour of the membranes as well as surface area determination and XPS analysis for analysing the detailed binding interactions present inside the membranes.

The presence of functional group inside membrane matrix as well as polar group incorporation can be also verified by XPS analysis (Figure S10). The comparison between the survey spectra of P, PC, PIL and PCIL0 membranes has been done (Figure S10A) which confirmed the introduction of nitrogen containing groups into the membranes as PC, PIL and PCIL0 have peak for N1s which is absent in case of P. In high resolution scan, while the spectra are deconvoluted we have found different peaks for different elements corresponding to different chemical moieties in the membranes. Figure 11B shows the deconvoluted spectra for membrane P, where C1s spectra shows peaks at 286.2 eV, 285 eV, 284.35 eV and 283.85 eV which corresponds to C-O-C, C=C/C-S, C-C and C-H carbons respectively[6]. For O1s, the peaks obtained at 533.5 eV and 532.2 eV for oxygens in S=O and C-O-C groups respectively. The S2p spectra shows peaks at 169.1 eV and 167.95 eV which are responsible for S=O and C-S sulfurs respectively. Figure 11C, 11D and 11E shows the deconvoluted high resolution scan

spectra for PC, PIL and PCIL0 membranes respectively. In PC membrane C1s spectra shows 5 peaks at 286.4 eV, 285.25 eV, 284.7 eV, 284.1 eV and 283.7 eV which represents C-O-C, C-N, C=C/C-S, C-C and C-H carbons respectively. In N1s deconvolution two peaks are witnessed at 400.5 eV and 399.9 eV for N-C and N-H nitrogen respectively[7]. These nitrogen peaks arise due to the ethane- 1, 2- diamine moiety incorporation. In PIL membrane (Figure S10D) also N1s spectra shows peaks for N-C and N-H nitrogens that obtained as a result of introduction of nitrogen containing ionic liquid into membrane matrix. Similarly, in case of PCIL0 (Figure S10E) respective peaks for carbon, nitrogen, oxygen and sulfur are obtained at different binding energies indicating the presence of these elements and their bonding with other elements.

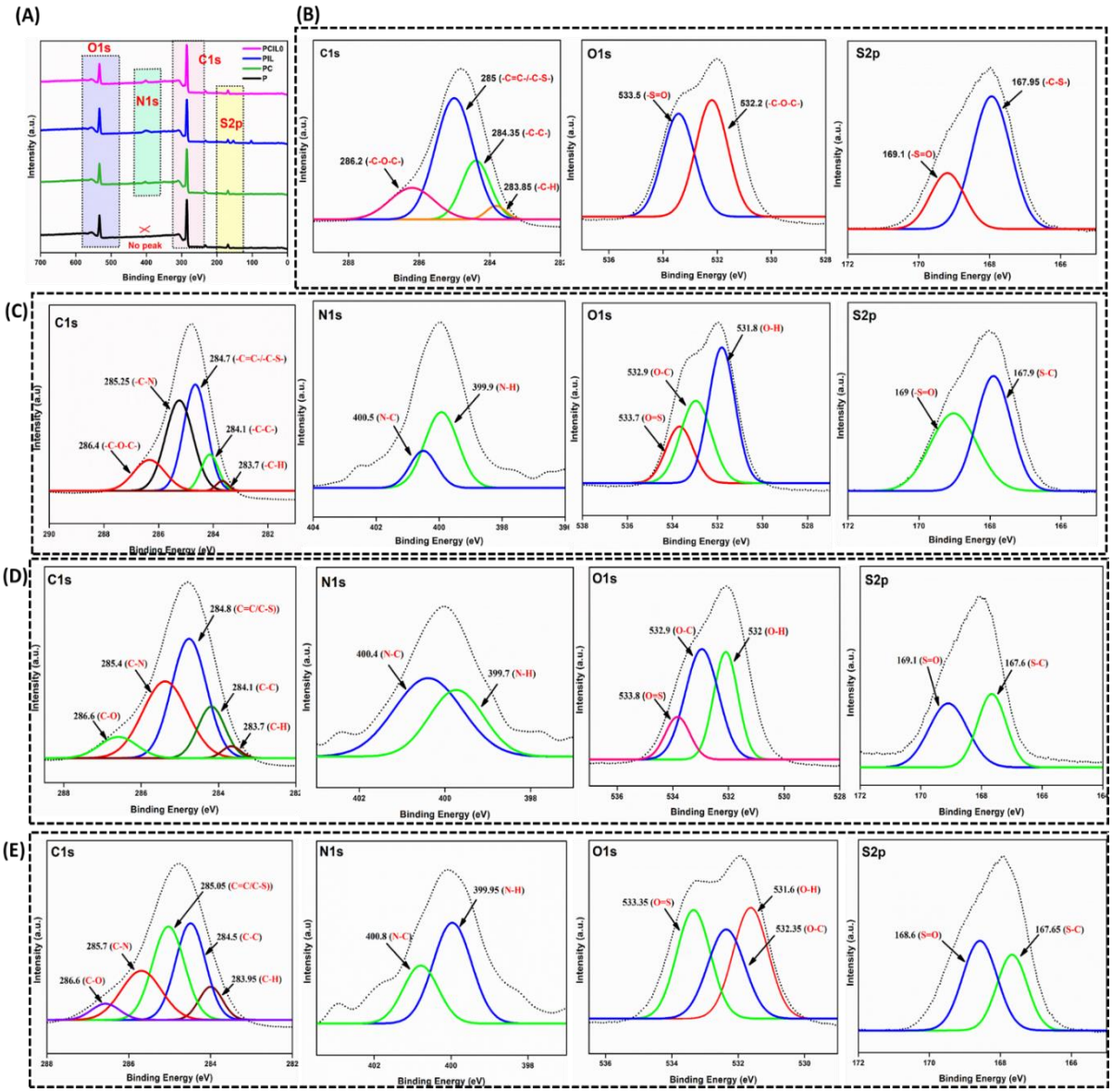

Figure S10: XPS (A) survey spectra of P, PC, PIL and PCIL0 membranes and high resolution scan XPS deconvolution data of C1s, O1s, N1s and S2p of (B) P, (C) PC, (D) PIL and (E) PCIL0 membranes

The changes in surfaces of the membranes have been witnessed in the FESEM images shown in Figure S11 at different diameter ranges. Our requirement is to prepare dense membranes. At first in P and PC membranes, few pores have been witnessed but after IL incorporation the membrane surfaces shows no prominent pores. The cross-sectional view of the membranes in Cross the cross-sectional images, the pore structures inside the membrane are witnessed to be

changing in each case. From the cross sections, the most packed porous structure is observed in case of PCIL-2 membrane. Although some pores are still witnessed inside the membrane, we have tried another approach to prepare a pore less membrane via spray coating of IL obtaining PC@IL membrane, whose surface and cross section both indicate a dense structure with defect free surface.

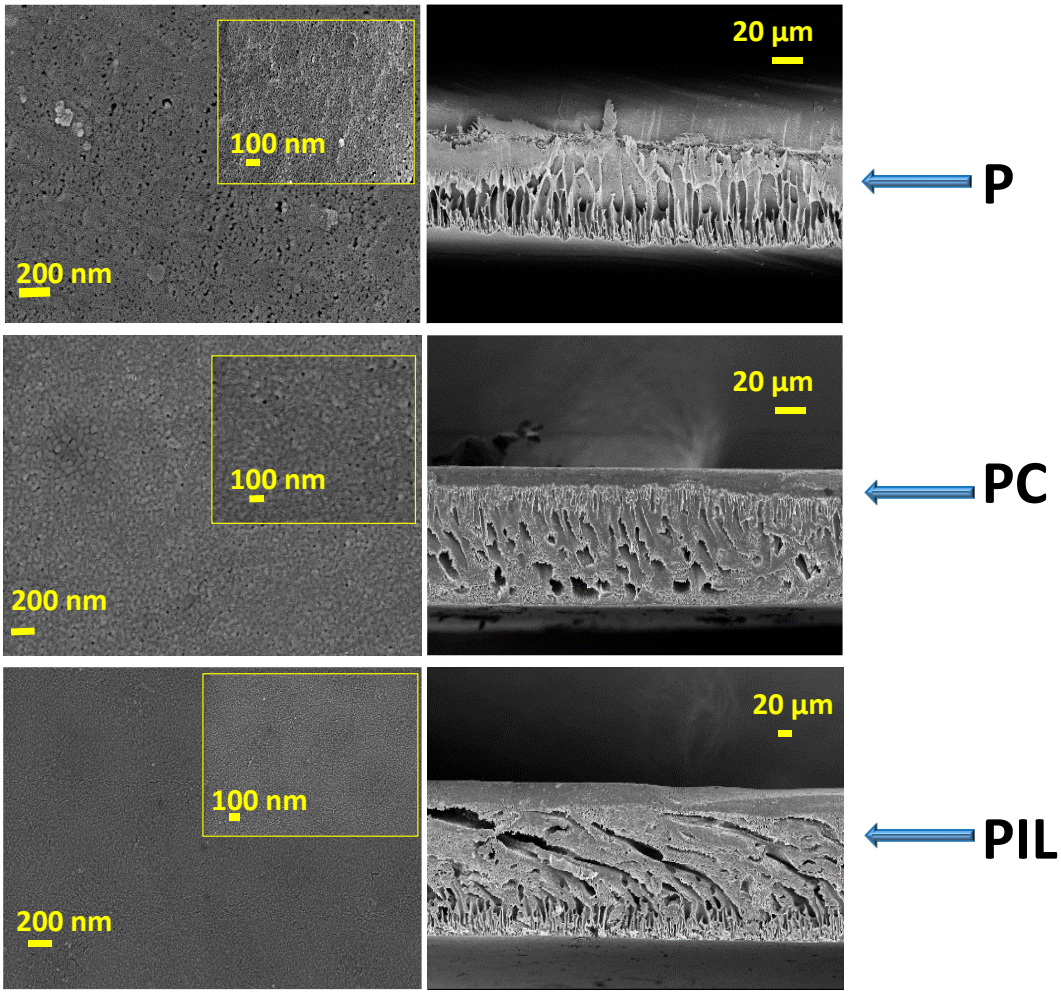

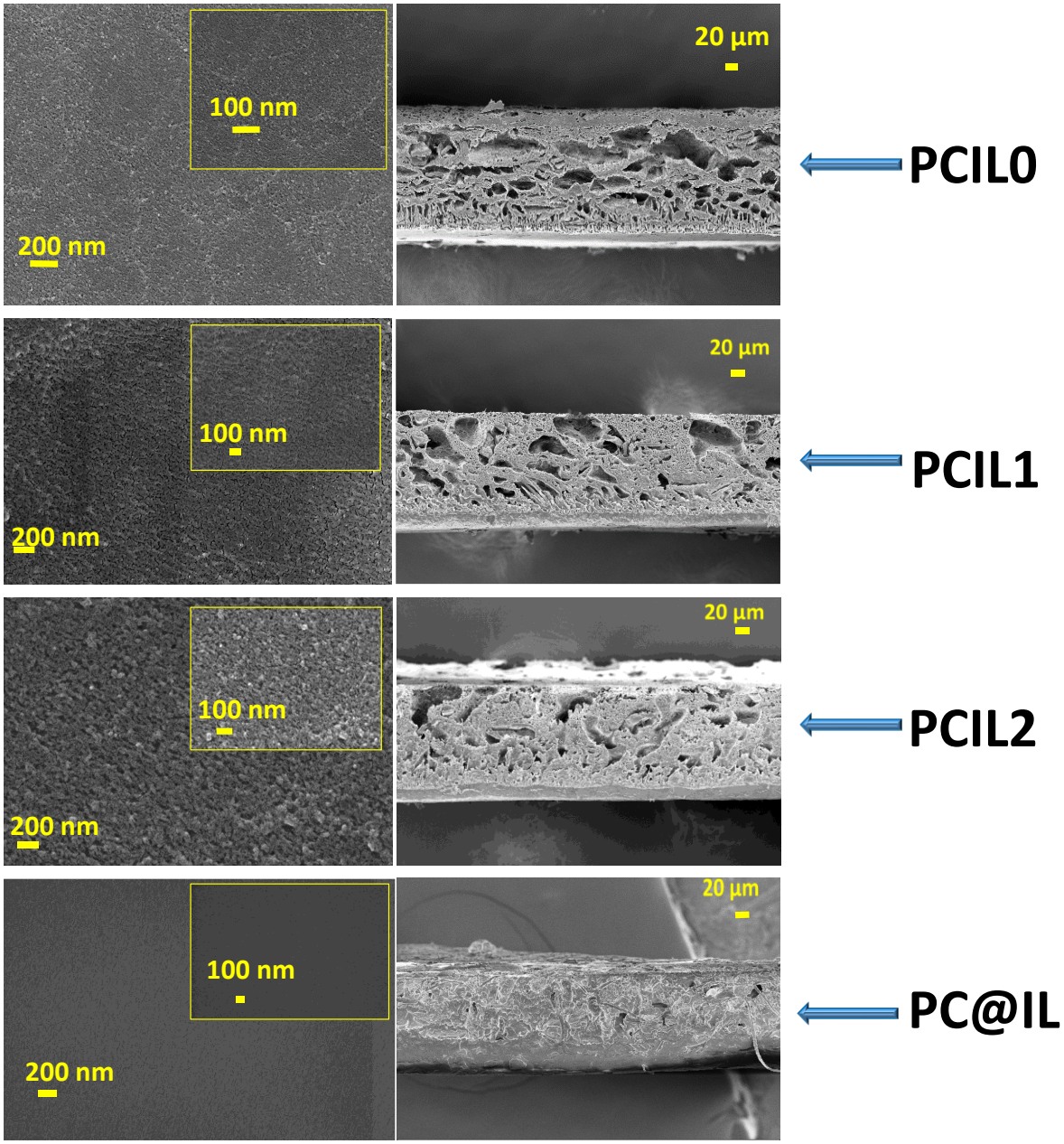

Figure S11: FESEM surface and cross-section images of different membranes

The pore-size distribution for PCIL2 and PC@IL membranes are shown in Figure S12. It has been witnessed that the pore size of PCIL2 membrane is higher than that in PC@IL. The decrease in pore size in the later one is due to the pore occupancy by IL.

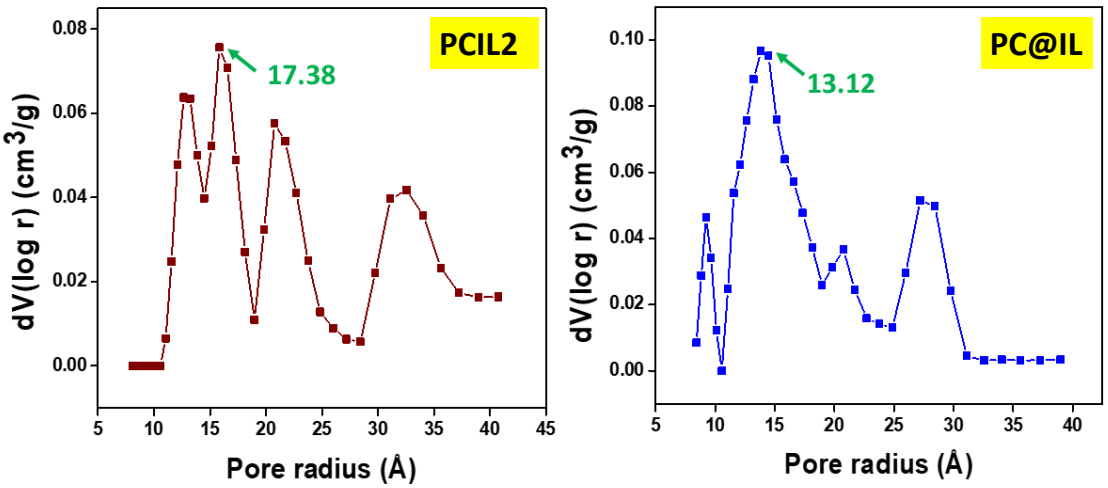

Figure S12: Pore size distribution curve of PCIL2 and PC@IL membranes

Another property of membrane is surface roughness, which has been determined via AFM analysis (Figure S13). For the bare polysulfone membrane P, roughness parameter Ra is obtained to be 8.07 nm. For PC and PIL membrane Ra values have been found to be 11.7 nm and 6.2 nm respectively. The increase in roughness in case of PC is due to the incorporation of CNC-NH_2 and in PIL the liquid nature of ionic liquid is responsible for the decrease in Ra value. In case of PCIL0, PCIL1 and PCIL3 membranes, Ra values obtained are 8.9 nm, 17.57 nm and 22.44 nm. This increasing trend in Ra values can be explained with increase in CNC-NH_2 content in the membrane matrix. In case of PC@IL membrane, due to spray coating of the surface by IL, the surface roughness value is witnessed to be decreased to 6.67 nm. It indicated a smooth surface of the membrane with a CO_2 selective IL layer.

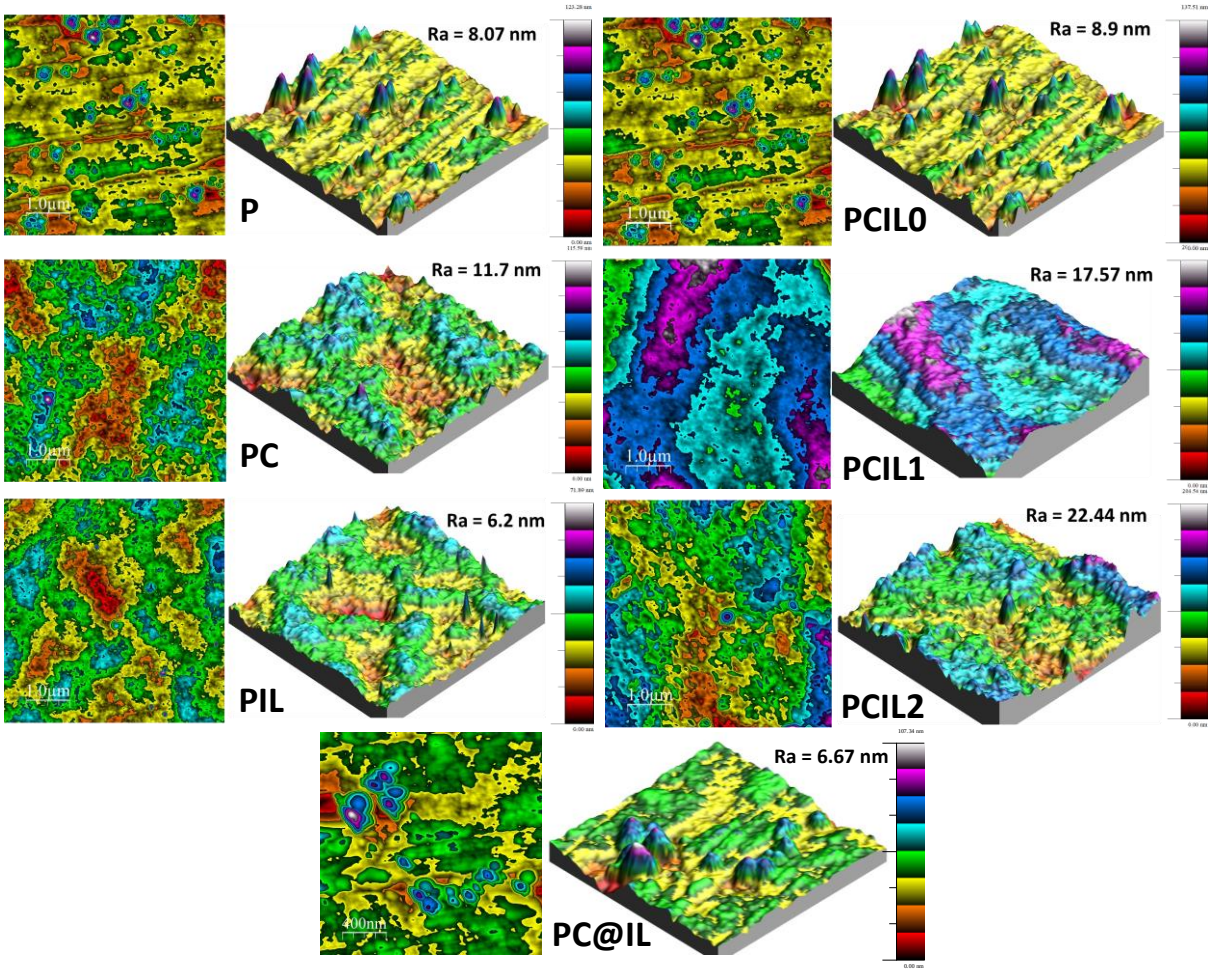

Figure S13: AFM images of all the membranes 2D and 3D views

From the comparison of FTIR spectra of P, PC, PIL and PCIL0 membranes, an appearance of peak at around 3400 cm^{-1} in all other membranes besides pristine polysulfone membrane (P) has been witnessed which indicates the presence of O-H and N-H stretching vibrations[8] (Figure S14). Peaks at 2936 cm^{-1}, 2949 cm^{-1} and 2921 cm^{-1} for PC, PIL and PCIL0 respectively have been obtained as a result of C-H stretching vibration of hydrocarbon chain present in CNC-NH_2 as well as IL. The peaks at around 1580 cm^{-1} and 1230 cm^{-1} have been corresponded to the C-O-C stretching and aromatic C-C stretching vibrations respectively[9].

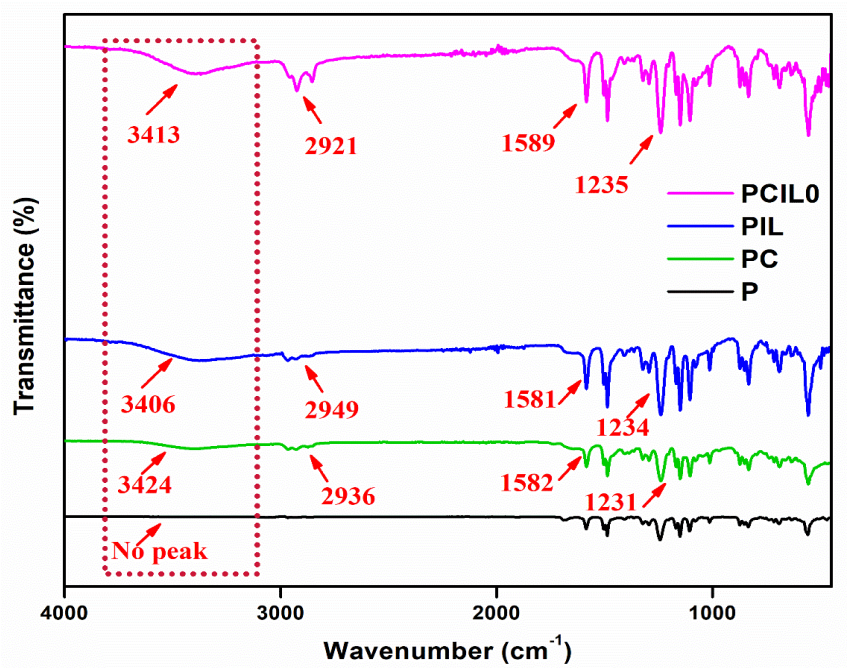

Figure S14: FTIR spectra of P, PC, PIL and PCIL0 membranes

Thermal stability of the membranes has been also studied and comparative weight degradation graphs of P and PCIL2 membrane are shown in Figure S15. After incorporation of CNC-NH_2 and ionic liquid, degradation at three different positions were observed. 1st degradation at 220.8 ºC arises due to degradation of CNC-NH_2 moiety[4], 2nd degradation at 283 ºC was for ionic liquid degradation[1] and the 3rd degradation at 518 ºC stands for degradation of polysulfone which can be correlated with the degradation of pristine polysulfone at 516 ºC. Thus, the best membrane PCIL2 has found to be thermally stable up to >200 ºC.

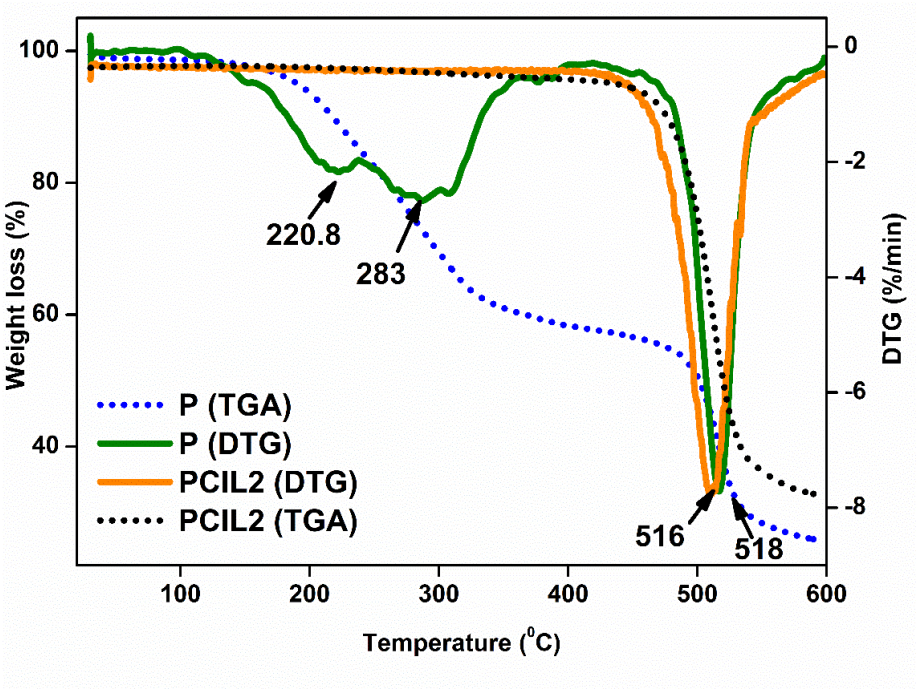

Figure S15: TGA and DTG analysis plot of P and PCIL2 membranes

One major intrinsic property of membrane is its mechanical property. The mechanical strength of the prepared membranes have been done with the help of a UTM and tensile strength of the membranes are evaluated as ultimate stress (Figure S16). The pristine polysulfone membrane possessed highest mechanical strength among other membranes with ultimate stress value of 4.28 MPa. On introduction of CNC-NH_2, the tensile strength values have been decreasing. For IL incorporated membrane PIL, tensile strength (3.17 MPa) is more than CNC-NH_2 incorporated one i.e., PC membrane (2.9 MPa). For PCIL0, PCIL1, PCIL2 and PCIL3 membrane, tensile strength values obtained are 2.48, 2.35, 2.04 and 0.92 MPa respectively. The PCIL3 membrane has least mechanical strength thus the maximum amount of CNC-NH_2 content has been optimized to be 0.08 % (w/v) which is the PCIL2 membrane. Although the tensile strength of the membranes gradually decreased upon addition of CNC-NH_2 and IL, the mechanical strength obtained are good enough to fulfill the purpose of the work. The newly prepared membrane PC@IL shows tensile strength of 3.42 MPa. Spray coating of IL on PC

membrane increase its original tensile strength from 2.9 MPa to 3.42 MPa which may be due to the probable hydrogen bonding of IL with CNC-NH_2 and PSF.

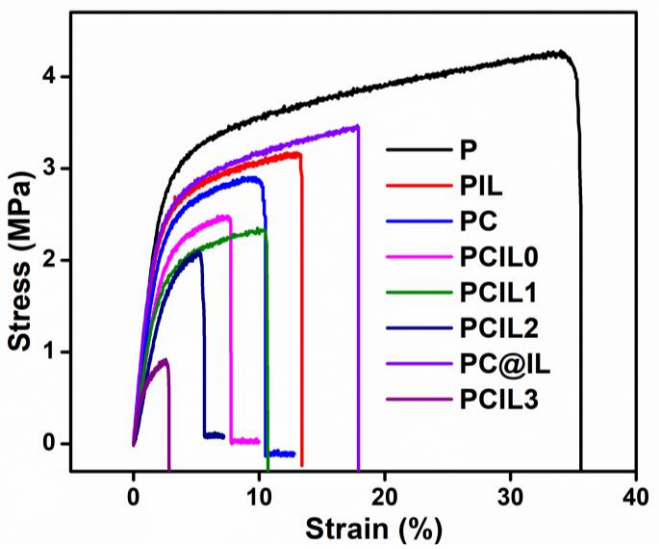

Membrane	Ultimate stress (Mpa)
P	4.28
PIL	3.17
PC	2.9
PCIL0	2.48
PCIL1	2.35
PCIL2	2.04
PC@IL	3.42
PCIL3	0.92

Figure S16: Stress Vs Strain graph of the prepared membranes and their ultimate stress

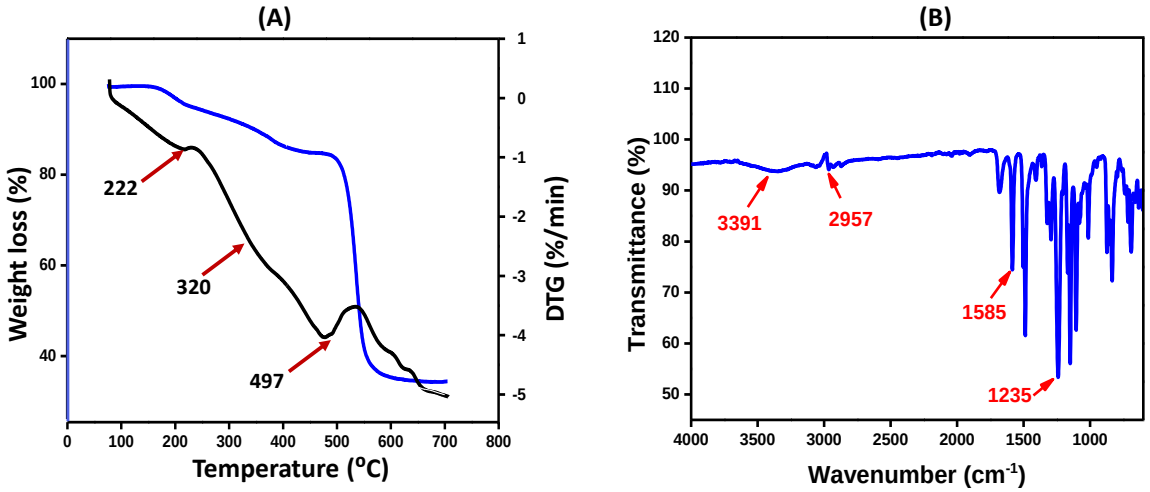

Figure S17: (A) TGA and DTG analysis of PC@IL membrane, (B) FTIR analysis of PC@IL membrane

Figure S17(A) shows the degradation points of different components of PC@IL membrane i.e., 222 ºC is for degradation of IL, around 320 ºC a broad ranged peak is obtained for CNC-NH_2 degradation. The degradation temperature of CNC-NH_2 increases than that of raw CNC-NH_2

due to occurrence of different interactions of functional groups with IL and polymer. At 497 ºC degradation peak arises due to thermal decomposition of polysulfone. Figure S17(B) shows the FTIR spectra of newly synthesized PC@IL membrane which shows similar characteristic peaks with the PCIL2 membrane.

Gas Permeability Measurement:

Using Equation S2, CO_2 permeability of the PCIL2 and PC@IL membranes are calculated in terms of pressure and flow rate (Figure S18). The variation in permeability of both membranes shows similar trend to permeance.

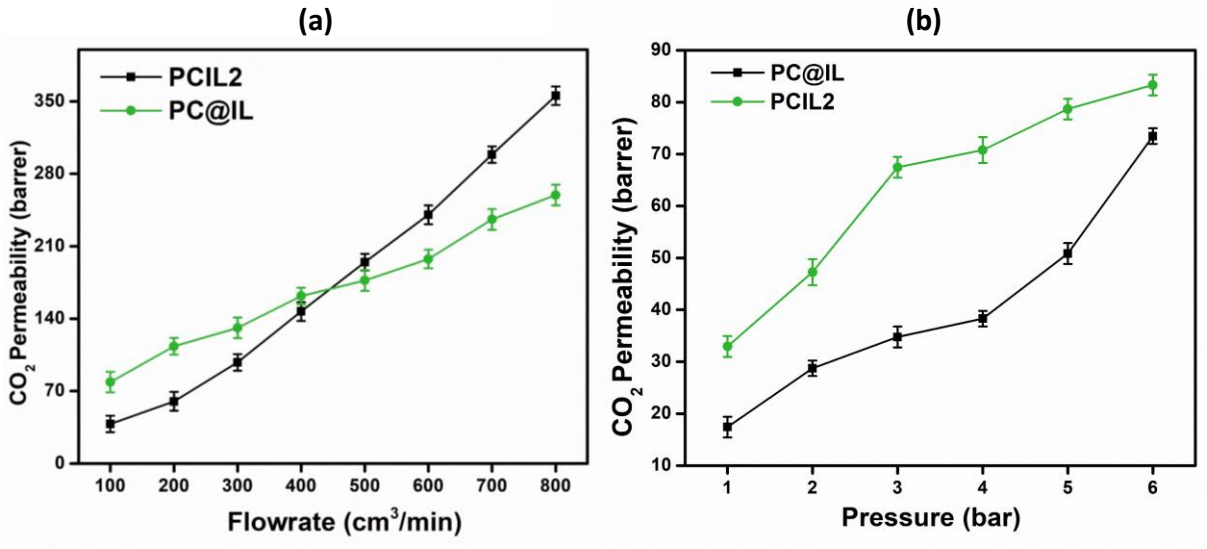

Figure S18: (a) CO_2 permeability of PCIL2 and PC@IL membranes a different flow rate, (b) CO_2 permeability of PCIL2 and PC@IL membranes at different pressures.

Structural changes in membranes under long time experiment at high pressure:

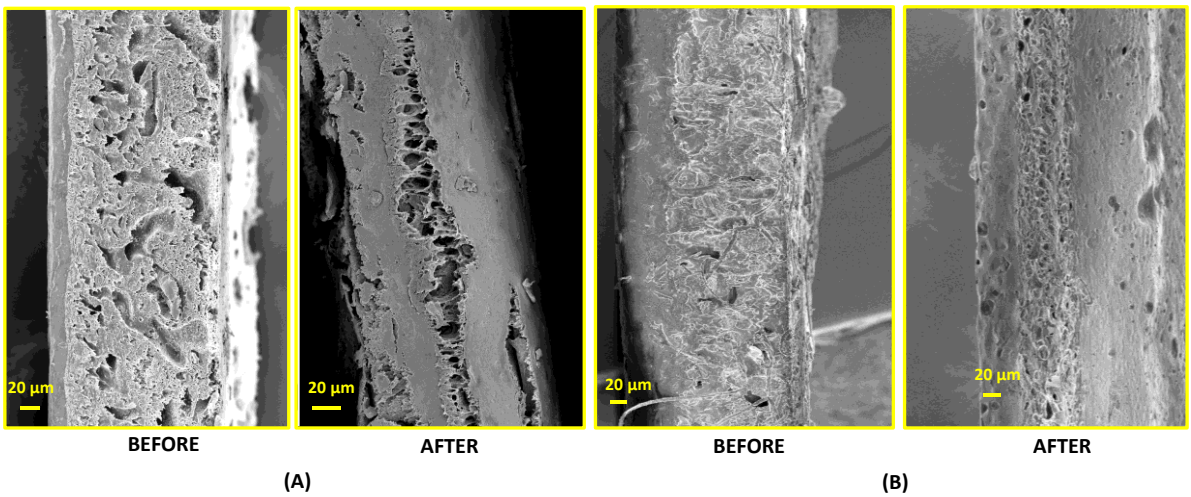

Figure S19: Cross sectional view of (A) PCIL2 and (B) PC@IL membranes before and after permeation

All the membranes have been subjected to gas permeation experiment at high pressure for long time. Their structural change after exposure to high pressure environment and after interaction with gas molecules are need to be analysed. Thus, FESEM cross sectional view of PCIL2 and PC@IL membranes before and after gas permeation experiment at 4 bar pressure and after 240 hours of use have been taken as shown in Figure S19 (A) and (B) respectively. The structures have been changed by exposure to high pressure for long time which is responsible for slight increase in permeability and selectivity decrease over time.

Involved reactions:

The reaction of amines with CO_2 resulting in reversible carbamate ionic complex is shown in Reaction S1.

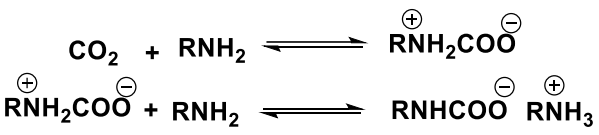

(Reaction S1)

The nucleophic attack of OH^- anion on CO_2 is demostrated in Reaction S2 where formation of reversible bicarbonate intermediate helps in Selective CO_2 permeation.

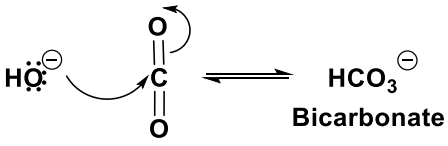

(Reaction S2)

Theoretical study:

Theoretical approach has been done to see the affinities of IL and CNC-NH_2 towards CO_2 and N_2. Figure S20 shows the corresponding interactions and binding energies of CO_2 and N_2 with hydroxide ion of IL and amine group of CNC-NH_2. The structures of IL, CNC-NH_2, CO_2 and N_2 have been optimized using semi empirical AM1 level of calculation. The optimized structure of the CO_2 and N_2 have been placed separately in the vicinity of the optimized IL and CNC-NH_2 respectively. They are also optimized using same level of calculations and the optimized structures are shown in Figure S20. The result obtained is similar to the order of gas solubility in IL 1-hexyl-3-methyl-pyridinium bis (trifluoromethylsulfonyl) imide[10] found by Anderson *et al* i.e., $N_2<CO_2$.

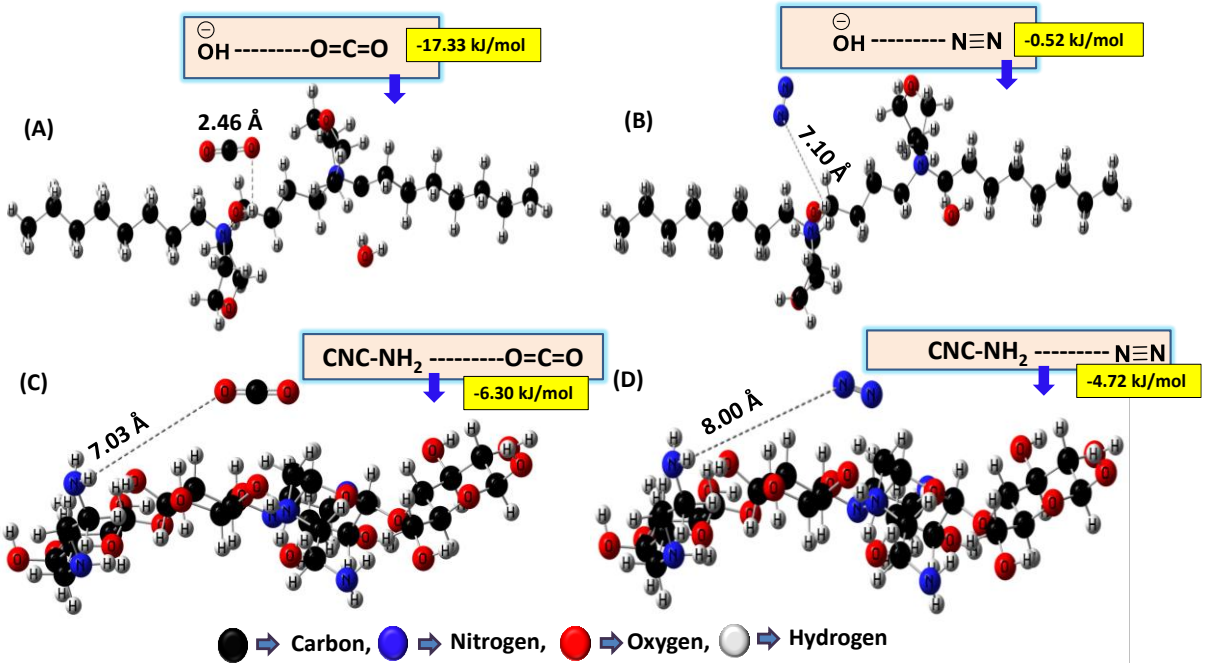

Figure S20: Optimized structure of (a) CO_2 in the vicinity of IL and (b) N_2 in the vicinity of IL (a) CO_2 in the vicinity of CNC-NH_2 and (b) N_2 in the vicinity of CNC-NH_2

Table S3: A comparison of reported literature with current study

Membrane type	**ILs**	**P (CO_2) (Barrer)**	**α (CO_2/N_2)**	**Test condition (bar, ºC)**	**Reference**
ILCM	EMIMDCA	514	20.5	0.13, 35	11
SILM	[emim][Tf_2N]	540.6	33.4	0.35, 25	12
PILM	[C_4vim][Tf_2N]	5.2	19	- , 293	13
PVAm	-	197	23.3	2, 25	14
PEI/PVA/PEG	-	260	22	1, 25	15
PIL4 : A1 : A2 : A3 : A4 : A5 : A6	-		29 17 32 34 11 14	2, RT	16
PILM	[DPyDBzPBI-BUI][Br] [DPyDBzPBI-BUI][BF_4] [DPyDBzPBI-BUI][Tf_2N] [DAnDBzPBI-BUI][Br] [DAnDBzPBI-BUI][BF_4] [DAnDBzPBI-BUI][Tf_2N]	23.9 30 36.2 15 25.1 30.9	21.5 22.7 20 24.2 27.3 21.6	-	17
PILM	[Tet(Im+)Benz][Tf_2N]	28.3	19.2	3, 20	18

IL-CS	[emim][Ac]	1146	3	- , 25	19
ZA/PTMSP	-	10,184	25	-, 25	19
Pervap 4060	-	47,376	10	-, 25	19
PCIL2	[Nbmd][OH]	355	10.73	4, RT	This work
PC@IL	[Nbmd][OH]	259.5	21.3	4, RT	This work

*ILCM = Ionic liquid composite membrane, SILM= Supported ionic liquid membrane, PILM = Poly (ionic liquid) membrane, PEI = Polyethylene imine, PVA = Polyvinyl chloride, PEG = Polyethylene glycol, CS = Chitosan, ZA = Zeolite 4A, PTMSP = Poly(trimethyl-1-silylpropyne), RT = Room temperature, P = Permeability, α = Selectivity.

In this study, the combined effects of morpholinium ion and hydroxide are employed to study membrane CO_2 permeability and CO_2/N_2 selectivity. The most effective membrane is impregnated with waste paper-derived CNC-NH_2, which aids in the uniform coating of the ionic liquid over the membrane. It is innovative to use this method to offer a selective membrane for CO_2 solubilization and facilitated transport. Metal cations have been employed for CO_2 capture in numerous recent studies. But our strategy offers a metal-free, environmentally beneficial separation process. Many published research struggle to achieve high selectivity and permeability simultaneously; in other words, the issue is that a membrane with high selectivity has lower permeability, and vice versa. Our developed membrane is capable of long-term permeability and good selectivity.

Author contribution:

Prarthana Bora: Methodology, Software, Formal analysis, Investigation, Resources, Data curation, Writing – original draft, review & editing; **Chinmoy Bhuyan:** Formal analysis, Investigation, Data curation; **Parashmoni Rajguru:** Software, Data curation, Computational analysis; **Swapnali Hazarika:** Conceptualization, Visualization, Methodology, Validation, Resources, Writing review & editing, Supervision.

References:

1. A. Dutta, K. Damarla, A. Kumar, P. J. Saikia and D. Sarma, *Tetrahedron Lett.*, 2020, **61**, 151587.
2. E. E. Jaekel, S. Kluge, S. Tröger-Müller, M. Tutus and S. Filonenko, *ACS Sustainable Chem. Eng.* 2022, **10**, 12895−12905.
3. H. Chen, Lignocellulose Biorefinery Engineering, *Woodhead Publishing*, 2015, 37-86.
4. E. C. da Silva Filho, J. C. P. de Melo and C. Airoldi, *Carbohydr. Res.*, 2006, **341**, 2842–2850
5. K. Kim, P. G. Ingole, J. Kim and H. Lee, *Chem. Eng. J.*, 2013, **233**, 242-250.
6. C. Bhuyan, A. Konwar, P. Bora, P. Rajguru, and S. Hazarika, *J. Hazard. Mater*., 2023, **442**, 129955.
7. R.J.J. Jansen and H. Van Bekkum, *Carbon*, 1995, **33**, 8, 1021-1027.
8. Aoopngan, C., Nonkumwong, J., Phumying, S., Promjantuek, W., Maensiri, S., Noisa, P., Pinitsoontorn, S., Ananta, S. and Srisombat, L., *ACS Appl. Nano Mater.*, 2019, **8**, 5329-5341.
9. K.Singh, S. Devi1, H. C. Bajaj, P. Ingole, J. Choudhary and H. bhrambhatt, *Sep. Sci. Technol.*, 2014, **49**, 2630-2641
10. J. L. Anderson, J. K. Dixon and J. F. Brennecke, *Acc. Chem. Res.*, 2007, **40**, 1208−1216.
11. J. Y. Lim, J. K. Kim, C. S. Lee, J. M. Lee and J. H. Kim, *Chem. Eng. J.* 2017, **322**, 254–262.
12. L. Y. Kong, W. D. Shan, S. L. Han, T. Zhang, L. C. He, K. Huang and S. Dai, *ChemSusChem.*, 2018, **11**, 185–192.
13. G. Zarca, W. J. Horne, I. Ortiz, A. Urtiaga and J. E. Bara, *J. Membr. Sci.*, 2016, **515**, 109–114.
14. M. Sandru, T.J. Kim, M.B. Hägg, *Desalination*, 2009, 240, 298.
15. S. Ben Hamouda, Q. T. Nguyen, D. Langevin, S. Roudesli, *Comptes Rendus Chimie*, 2010, **13**, 372.
16. T.K. Carlisle, E.F. Wiesenauer, G.D. Nicodemus, D.L. Gin and R.D. Noble, *Ind. Eng. Chem. Res.*, 2013, 52, 1023–1032.

17. S.V. Shaligram, A.S. Rewar, P.P. Wadgaonkar and U.K. Kharul, *Polymer*, 2016, **93**, 30–36.
18. A. E. O'Harra, E. M. DeVriese, E. M. Turflinger, D. M. Noll and J. E. Bara, *Polymers*, 2021, **13**, 1388;
19. A., Fernández-Barquín, C. Casado-Coterillo and Á. Irabien, *Sep. Purif. Technol.*, 2017, **188**, 197-205.